# On the Design of High-Performance Surface-Mounted PM Motors

Gordon R. Slemon

*Abstract*— **This paper considers the major design factors which constrain the maximum acceleration capability of surface-mounted neodymium-iron-boron permanent magnet motors as used in servo drives. Expressions are derived for typical achievable values of the air-gap flux density and the linear current density around the stator periphery. For applications with small values of the duty factor, the stator linear current density is limited by the need to avoid demagnetization. For larger values of duty factor, the constraint is the ability of the cooling system to remove the heat losses within the magnet and insulation temperature limits.**

**The paper derives general approximate expressions for maximum torque and acceleration limits, and shows graphs from which the range of acceleration capability of a permanent magnet motor in a given application can be assessed. The constraints involved in matching the motor design to an inverter with given maximum voltage capability are also discussed.**

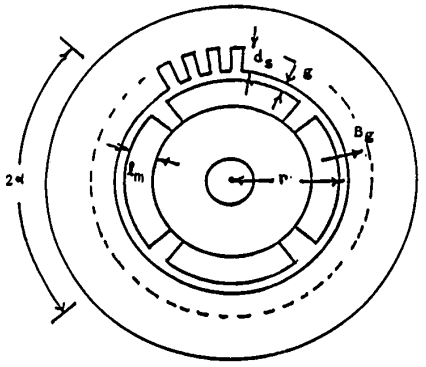


Fig. 1. Cross section of a 4-pole PM motor.

## I. Introduction

PERMANENT MAGNET (PM) motors using neodymium-iron-boron (Nd-Fe-B) magnets are particularly well suited for high performance, variable speed and position drives because of their high peak torque capability and their essentially linear relationship between torque and stator current [1, 2]. This paper presents some design relationships for such PM motors.

The specific application area targeted in this paper is the class of servo-drives such as encountered in robotics, machine tools and production materials handling, where there is a requirement for rapid precise excursion, followed by a period of relatively low torque demand, ie., a low load factor. The specification for such motors usually calls for a high peak torque $T$, combined with a low polar moment of motor inertia $J_m$ to achieve a rapid acceleration $\alpha$. This peak torque is to be available up to a base speed $\omega_b$. In some drives, a capability for speeds above $\omega_b$ with reduced torque is desired.

The major factors limiting the acceleration capability of a PM motor are the necessity of protecting the magnets from demagnetization, and the necessity to limit the temperature of both the magnets and the winding insulation. This paper examines these constraints in a general approximate way, and provides the reader with an indication of the range of ratings and performance criteria which can reasonably be achieved with these motors. Particular attention is given to extending the application of PM motors to higher torque and power ratings.

The PM motors considered in this paper are of the surface-mounted magnet type shown in cross section in Fig. 1. This structure provides radially-directed flux into a slotted stator. The stator windings are assumed to be nearly sinusoidally distributed and are supplied from a variable frequency source with controlled near-sinusoidal phase currents. This constraint on the type of supply is imposed to provide for dynamic control of the instantaneous angle between the rotor and stator fields. To the extent that the phase currents are near-sinusoidal and the winding distribution is also near-sinusoidal, this type of drive provides a torque which is relatively free of ripple.

## II. Flux Density Constraints

The torque of a PM motor can be expressed as [3],

$$T = 2\pi r^2 \ell B_{1g} K_{1s} \sin\beta \quad \text{N.m} \tag{1}$$

where $r$ is the rotor radius and $\ell$ is the rotor length. The rms value of the fundamental space component of the air gap flux density due to the magnet is $B_{1g}$, and the rms linear current density along the stator periphery is $K_{1s}$. The angle $\beta$ is the angular displacement between the fields produced by the magnet and the stator current.

The achievable value of $B_{1g}$ is constrained by the magnet properties and dimensions and by saturation in the stator teeth. A demagnetization characteristic for Nd-Fe-B magnet material is shown in Fig. 2. It is characterized by an essentially linear relation with a residual flux density $B_r$ and a slope of approximately $\mu_o$ until a point $(B_D, H_D)$is reached, a limit which must not be exceed if demagnetization is to be avoided.

Paper JF 16–94, approved by the Electric Machines Committee of the IEEE Industry Applications Society for presentation at the 1992 Industry Applications Society Annual Meeting, Houston, TX, October 4–9. Manuscript released for publication June 2, 1993.

The author is with The Department of Electrical and Computer Engineering, University of Toronto, 10 King's College Road, Toronto, Canada, M5s 1A4.

IEEE Log Number 9213445.

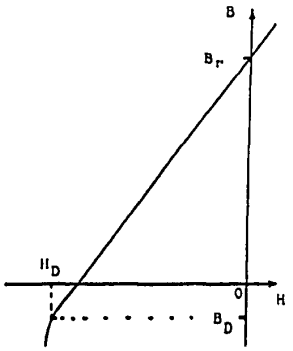


Fig. 2. Demagnetization characteristic for Nd-Fe-B magnet material.

The average flux density $B_{go}$ in the air gap due to the magnet alone is

$$B_{go} = \frac{\ell_m}{\ell_{ge}} B_r \quad \text{T} \tag{2}$$

where $\ell_m$ is the radial length of the magnet and $\ell_{ge}$ is the effective radial distance from the stator teeth to the rotor iron core, with appropriate provision for the usually small effect of stator slotting. The minimum value of the air gap $g$ above the magnet is set by mechanical considerations. An empirical expression is [4],

$$g \approx 0.0002 + 0.003\sqrt{r\ell} \quad \text{m} \tag{3}$$

For some high speed motors, it may be desirable to bind the rotor with glass or carbon fibre tape to hold the magnets against centrifugal forces. The usual range of $g$ is 0.5 to 1.5 mm.

Because the magnet has a relative permeability near unity, the effective length $\ell_{ge}$ is only slightly greater than the physical length $\ell_g = g + \ell_m$, the effect of Carters' coefficient being less than 5% in most designs [1]. The maximum flux density $B_t$ in the stator teeth is usually limited to about 1.6 $T$ to avoid excessive saturation. The desired value of air gap flux density above the magnet is then given by

$$B_{go} = \frac{w_t}{\lambda_s} \hat{B}_t \quad \text{T} \tag{4}$$

for a tooth width $w_t$, slot width $w_s$ and a slot pitch $\lambda_s = w_t + w_s$. For most machines, the slotting of the stator is such that $w_t \approx w_s$. Thus, a typical value for air gap density is about 0.8 $T$. With a residual flux density $B_r$ of about 1.1 $T$, the ratio $\ell_m/\ell_{ge}$ of eq. 2 is about 0.7 to 0.75. Thus, the magnet length can be as small as about 4 $g$. As an example, if $g$=1.0 mm, $w_s = w_t$=5.0 mm and $\ell_m$=4.0 mm, then $\ell_{ge} = 1.08\ \ell_g$=5.42 mm and $B_{go}$=0.81 T.

If each magnet spans an electrical angle of $2\alpha$, the fundamental sinusoidal space component of the air gap flux density is given by

$$B_{1g} = \frac{2\sqrt{2}}{\pi} B_{go} \sin\alpha \quad \text{T (rms)} \tag{5}$$

The angular width $2\alpha$ of the magnet is usually fixed in the range 120° to 140°. Increase beyond this range adds little to the effective density $B_{1g}$ but adds flux which must be carried by the stator yoke. Typically, for $\alpha = 60°$ and $B_{go} = 0.8T$, $B_{1g}$=0.63 T. The nature of the constraints on flux density are such that the value of $B_{1g}$ will be relatively constant over a wide range of motor torque ratings.

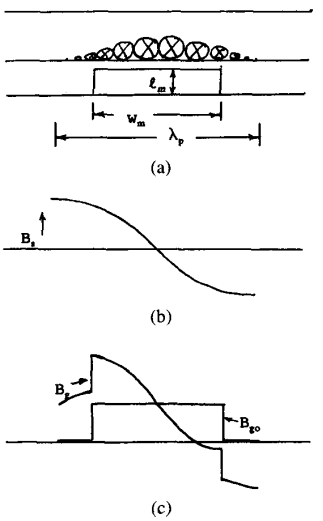


Fig. 3 (a) Sinusoidal current sheet above a rectangular magnet. (b) Flux density $B_s$ due to stator current. (c) Resultant flux density $B_g$.

## III. Design For Magnet Protection

When the motor is operated at maximum torque and stator current, the linear current density in the stator must be constrained so that no part of the magnet has its flux density reduced beyond the value $B_D$ as shown in Fig. 2. This value $B_D$increases with increased magnet temperature. With currently available Nd-Fe-B materials, a value of about $B_D = -0.2$T can be achieved at a temperature of 120°C.

Fig. 3(a) shows a sinusoidally-distributed stator current sheet located above a magnet in the angular position to create maximum torque, i.e. $\beta = 90°$. Acting alone on an effective gap of length $\ell_{ge}$, the stator current would produce a sinusoidally distributed gap flux density with maximum value [2],

$$\hat{B}_s = \frac{2\sqrt{2} r \mu_o K_{1s}}{p\ell_{ge}} \quad \text{T} \tag{6}$$

as shown in Figure 3(b) where $p$ is the number of poles. Adding this to the flux density distribution due to the magnet alone, as shown in Figure 3(c), results in an increase in the flux density $B_g$ at the leading end of the magnet, i.e. in the direction of rotor torque, and a decrease in flux density at the lagging end. The criterion for magnet protection is then, from eq. 2,

$$\hat{B}_s \sin\alpha \le \left(\frac{\ell_m}{\ell_{ge}} B_r - B_D\right) \quad \text{T} \tag{7}$$

Combining eq. 6 and eq. 7, the linear current density constraint is given by

$$K_{1s} \leq \frac{p\ell_{ge}\left(\frac{\ell_m}{\ell_{ge}}B_r - B_D\right)}{2\sqrt{2}r\mu_o \sin\alpha} \quad \text{A/m} \tag{8}$$

If saturation in the stator teeth is ignored, the effective flux density producing torque remains at the value $B_{1g}$ given in eq. 5, since the component $B_s$ is in space quadrature with $K_{1s}$ and produces no torque. The maximum available torque is then given, for $\beta = 90°$, using eq.1,2,5 and 8, as

$$\hat{T} = \frac{2r\ell p\ell_m B_r}{\mu_o}\left(\frac{\ell_m}{\ell_{ge}}B_r - B_D\right) \quad \text{N.m} \tag{9}$$

It will be noted that this maximum torque is proportional to $r$ and $\ell$, i.e. to the surface area of the rotor. The torque is proportional to the magnet length $\ell_m$ since a large path length for flux requires a larger stator current density value to produce the limiting value of flux density $B_s$. The maximum torque is found to be independent of the angular half width $\alpha$ of the magnet. The quantity in brackets in eq. 9 is relatively constant for a given magnet material and temperature. The maximum realizable torque may be reduced somewhat below the value given in eq. 9 due to magnetic saturation in the stator in the region of high flux density as shown in Fig. 3(c).

## IV. Constraint on The Number of Poles

The maximum torque $T$ is seen to be proportional to the number of poles $p$, as shown in eq. 9, since an increase in $p$ decreases the pole pitch $\lambda_p$ of Figure 3(a) and the width $w_m$ of each magnet over which the demagnetizing effect of $K_{1s}$ applies. For small machines, the maximum number of poles is limited by the minimum practical width of the stator teeth and slots. In general,

$$p = \frac{2\pi r}{3c(w_s + w_t)} \tag{10}$$

where $c$ is the number of slots/pole-phase. For a reasonably good approximation to a sinusoidal distribution, the value of $c$ should be 2 or greater. If the minimum tooth and slot widths are set at about 4 mm, the minimum radius for a 2-pole machine with $c$=2 is about 16 mm.

As the number of poles is increased, the maximum frequency of the supply inverter will also be increased for a given maximum drive speed. This will tend to increase the inverter losses. However, an increase in the number of poles decreases the flux which must be carried by the stator yoke and thus reduces the overall radius of a motor of a chosen gap radius.

## V. Inertia And Rotor Shape

The achievement of a high acceleration capability requires a high maximum torque combined with a low polar moment of inertia $J_m$ of the motor. In many servo applications, the mechanical load is coupled to the motor through a reduction gear of ratio $n$ . Maximum load acceleration is achieved when this ratio is so chosen that the load inertia $J_L$ is related to the motor inertia by

$$J_L = n^2 J_m \quad \text{kg.m}^2 \tag{11}$$

Thus, the total effective inertia is typically double that of the motor. It is therefore reasonable to use the rotor inertia alone in assessing the accelerating capability of the machine.

In many designs, the rotor may be modelled approximately as a solid cylinder of radius $r$, length $\ell$, with the density $\rho_i$ of iron. The somewhat lower density of the magnet material and of the filler which may be used in the spaces between magnets to reduce windage loss is assumed to compensate for the added inertia of the shaft ends and fans. The polar moment of inertia of the motor is then approximated by

$$J_m = \frac{\rho_i \pi r^4 \ell}{2} \quad \text{kg.m}^2 \tag{12}$$

Combining this with the maximum torque expression of eq. 9 gives the maximum available acceleration of the motor alone as

$$\alpha = \hat{T}/J_m = \frac{4pB_r\ell_m}{\pi\rho_i r^3}\left(B_r\frac{\ell_m}{\ell_{ge}} - B_D\right) \quad \text{rad/s}^2 \tag{13}$$

For some large radius machines, a somewhat lower inertia may be achieved by use of a hollow rotor with spokes.

While the acceleration expression of eq. 13 does not contain the rotor length $\ell$, it should not be concluded that the acceleration is independent of $\ell$. From eq. 9, the product $r\ell$ is constant for a specified maximum torque rating. Thus, for high acceleration, the rotor length should be chosen as large as is practical. Mechanical considerations limit the maximum value of the ratio $y = \ell/r$. The critical speed of the rotor is proportional to $r/\ell^2 = 1/ry^2$ [5]. This critical speed should be at least 20% above the maximum speed required of the motor. Normally, the ratio $y$ for high performance machines is limited to about 6.

Consider a range of motors for which the magnet material is characterized by $B_r = 1.1\text{T}$, $B_D = -0.2\text{T}$. The half-angular width of the magnets is fixed at 60°, and the air gap is adjusted to keep the ratio $\ell_m/\ell_{ge}$ constant at 0.74. The slots per pole-phase is set at $c$=2. The density of the rotor is taken as 7600 kg/m$^3$. The torque expression of eq. 9 then is simplified to

$$\hat{T} = 1.78r^2 yp\ell_m \quad \text{MN.m} \tag{14}$$

For this case, the acceleration is given by

$$\alpha = 150\frac{p\ell_m}{r^3} \quad \text{rad/s}^2 \tag{15}$$

Figure 4 shows a set of relations giving the maximum angular acceleration $\alpha$ achievable from machines with maximum torque capability $T$ up to 1000 N.m, for 6 sets of values of $p$, $\ell_m$, and $y$. All of these curves are within the constraint on the number of poles given in eq. 10 for a slot pitch $\lambda_s$ =8 mm. As would be expected, the acceleration capability decreases as the torque rating is incresaed. Any increase in the number of poles, the $\ell/r$ ratio of the rotor or the magnet thickness increases the maximum acceleration. For the unloaded motor of Curve 4 with maximum torque of 500 N.m and with ideal current supply from its inverter, a speed of 400 rad/s (3820 rev/min) could be achieved in 10 ms.

For motors of lower maximum torque rating, a 2-pole construction would normally be used. Figure 5 shows $\alpha - T$

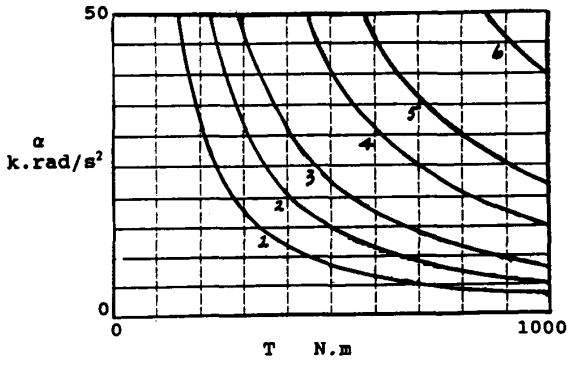


| Plot | y | p | $\ell_m$ (mm) |
|---|---|---|---|
| 1 | 4 | 4 | 4 |
| 2 | 6 | 4 | 4 |
| 3 | 4 | 6 | 4 |
| 4 | 6 | 4 | 6 |
| 5 | 4 | 6 | 6 |
| 6 | 6 | 6 | 6 |

Fig. 4. Maximum angular acceleration $\alpha$ for motors with maximum torque $T$.

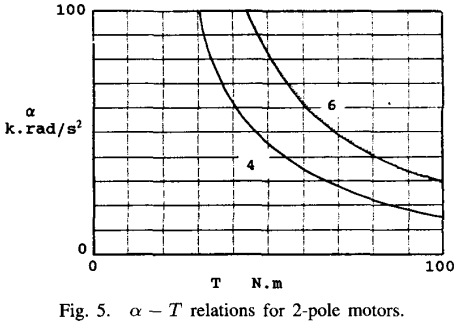


Fig. 5. $\alpha - T$ relations for 2-pole motors.

relations for two values of the ratio $y$ with $\ell_m$ =4 mm in the torque range up to 100 N.m.

## VI. Cooling Capability Constraint

Acceleration values such as are shown in Figures 4 and 5 are achievable only to the extent that the motor temperature limits are not exceeded at the required duty cycle of the drive. Provision must be made to keep the temperature of the magnets below about 120°C for currently available Nd-Fe-B materials and to keep the stator insulation temperature below about 130°C for the commonly-used Class B materials. This requires means of removing the heat produced in the stator winding and the stator iron. Generally, losses in the rotor materials can be considered to be negligible except for very high frequency operation [6].

The power loss in the stator winding may be approximated by considering the conductor to be concentrated into an equivalent solid cylindrical sheet at the stator surface. Of the total stator periphery of a parallel-sided slot configuration, a fraction $\gamma = w_s/\lambda_s$ is available for conductors. The slot area $A_s$ can then be expressed as

$$A_s = 2\pi r d_s \gamma \quad \text{m}^2 \tag{16}$$

where the ratio of slot depth $d_s$ to the slot width $w_s$ is usually 4 or larger. For smaller machines, a more typical stator has a parallel-sided tooth configuration and an appropriate adjustment may be made.

The ratio of the actual conductor area to the slot area is the space factor $f_s$ which typically has a value in the range 0.3 to 0.5. The equivalent depth $d_e$ of the cylindrical conductor sheet can now be expressed as

$$d_e = f_s d_s \gamma \quad \text{m} \tag{17}$$

The length of the equivalent cylindrical sheet of conductor may be estimated by noting that the end turn of a full-pitched coil spans a peripheral distance of $1/p$ of the stator circumference. For short pitched coils, this span is somewhat reduced. The equivalent length $\ell_c$ of solid conductor can be expressed approximately as

$$\ell_c = \ell + \sigma \frac{2\pi r}{p} \quad \text{m} \tag{18}$$

where $\sigma$ is the ratio of the actual length of the overhang portion to the pole pitch making provision for the necessary diamond shape of the coil. This factor is typically in the range 1.5 to 2.0.

The actual linear current density $K_s$ in the stator is related to the effective sinusoidally-distributed value $K_{1s}$ by

$$K_{1s} = k_w K_s \quad \text{A/m} \tag{19}$$

where $k_w$ is the winding factor made up of distribution and pitch factor components [7]. Typically, the winding factor for windings with $c$ =2 or 3 is between 0.93 and 0.97.

The power loss $P_{sw}$ in the stator windings may now be expressed as

$$P_{sw} = \frac{\rho_c 2\pi r \ell_c K_{1s}^2}{d_e k_w^2} \quad \text{W} \tag{20}$$

where $\rho_c$ is the conductor resistivity at the operating temperature.

The other significant loss in the machine is core loss in the stator teeth and yoke. In PM machines, the eddy current part of this loss is proportional to the square of the both the flux density and the frequency. In the teeth, it is also approximately proportional to the square of the number of slots per pole, i.e. to $c^2$ [8] because of the rapid change of flux density in the teeth located at the ends of the magnets. Designs with relatively low values of slots per pole-phase of $c = 2$ or 3 are therefore preferred. Typically, the motor stator might be designed to give flux density values in the teeth and yoke so that the average stator core loss is made roughly equal to the average loss in the stator conductors.

In order to gain insight into the limitations imposed on the maximum available torque by these losses, let us consider a simple model of the cooling capability. Most PM motors are of the totally enclosed fan cooled (TEFC) type. This construction is preferred to protect the magnets from iron dust and corrosive gases and to avoid contamination of the stator insulation. The

motor is cooled by forced circulation of air over the outer surface of the stator. The cooling capability can be expressed as

$$P_L = Ah\Delta T \quad \text{W} \tag{21}$$

where $A$ is the available cooling surface area. The cooling coefficient h can be approximated empirically by [4],

$$h = 20\nu^{0.6} \quad \text{W/°C.m}^2 \tag{22}$$

where $\nu$ is the air velocity in m/s. The temperature difference $\Delta T$ is that between the cooling surface and the cooling air. Typically, the maximum stator temperature would have to be restricted to about 100°C, while the ambient temperature of the air might be as high as 40°C depending on the application.

As a rough approximation, let us assume that the available cooling area $A$ is twice the outer surface area of the equivalent stator conducting sheet at the air gap, i.e.,

$$A = 2(2\pi r\ell_c) \quad \text{m}^2 \tag{23}$$

Using the assumption of equality of the average conductor losses and iron losses,

$$P_L = 2P_{sw_{(\text{avg})}} \quad \text{W} \tag{24}$$

Consider a drive application with a duty cycle such that maximum torque is required for a fraction $f_d$ of the time with substantially no torque requirement and thus no significant stator winding loss for the remainder of the time. Also assume that the period of this cycle is short enough that the motor temperature remains essentially constant. For this condition, the average loss in the stator conductor can be expressed as

$$P_{sw_{(\text{avg})}} = f_d P_{sw_{(\max)}} \quad \text{W} \tag{25}$$

For more complex duty cycles, the load factor $f_d$ may be evaluated as the square of the ratio of rms to peak torque over the cycle period.

Combining these expressions provides an estimate of the maximum acceptable value of the linear current density in the stator as

$$K_{1s_{(\text{avg})}} = \left(\frac{d_e k_w^2 h\Delta T}{\rho_c f_d}\right)^{\frac{1}{2}} \quad \text{A/m} \tag{26}$$

Typically, the temperature difference $\Delta T$ might be 60°C. With an air velocity $v$ of 10 m/s, the cooling coefficient $h$ is about 80 W/° C.$m^2$. The winding factor may be assumed to be about 0.95. At a winding temperature of 120°C, the conductor resistivity $\rho_c$ is $2.4\times10^{-8}\Omega.m$. For these conditions, the allowable linear current density is limited to

$$K_{1s} = 0.43\left(\frac{d_e}{f_d}\right)^{\frac{1}{2}} \quad \text{MA/m} \tag{27}$$

The linear current density is also subject to the limit required for magnet protection. From eq. 8, with $B_r = 1.1\text{T}$, $B_D = -0.2\text{T}$, $\ell_m/\ell_{ge} = 0.74$ and $\alpha = 60°$, this constraint is

$$K_{1s} = 0.45\frac{p\ell_m}{r} \quad \text{MA/m} \tag{28}$$

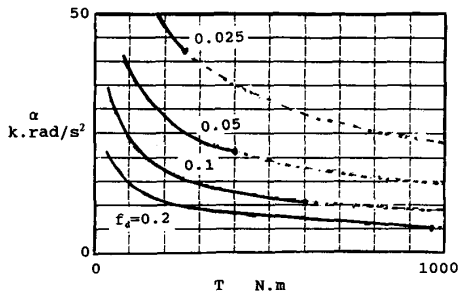


Fig. 6. Maximum acceleration $\alpha$ of motors of maximum torque $T$ for values of duty factor $f_d$. $p = 4$. $\ell_m = 4$ mm.

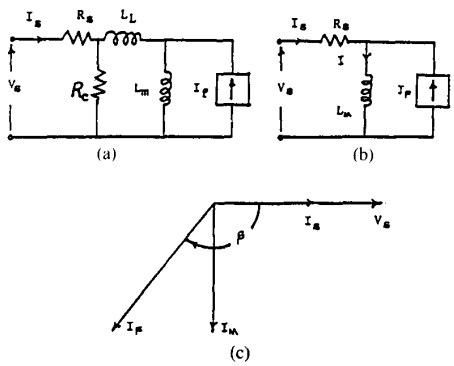


Fig. 7. (a) Equivalent circuit for PM motor. (b) Simplified equivalent circuit. (c) Phasor diagram for unity power factor.

The appropriate value of $K_{1s}$ may now be inserted in eq. 1 to obtain the following expression for the maximum available torque.

$$T = 3.95r^3 yK_{1s} \quad \text{N.m} \tag{29}$$

Fig. 6 shows limiting values of achievable angular acceleration for motors with maximum torque capability up to 1000 N.m, for four values of load factor $f_d$, with $B_r = 1.1T, B_D = -0.2T, \ell_m/\ell_{ge}$=0.74 and $\alpha = 60°$. The solid lines indicate the regions of thermal limitation at each load factor. These terminate on the dotted line which is the limit imposed by magnet protection. As the load factor is increased, the thermal constraint is seen to be the dominate limit on acceleration.

## VII. Matching To Inverter

Up to this point, no mention has been made of the level of the supply voltage and current. These are characteristic of the available power supply, the inverter and the drive rating. In this section, some of the major equivalent-circuit parameters of the motor will be expressed in terms of motor dimensions as an aid in designing a motor with specified parameters to match an available inverter source.

Fig. 7(a) shows a conventional steady-state equivalent circuit for a PM motor [6, 7]. The magnet is represented by an alternating current source $I_f$, where

$$I_f = \frac{2p\ell_{ge}B_{1g}}{3\mu_0 N_{se}} \quad \text{A} \tag{30}$$

where the equivalent number of sinusoidally-distributed turns $N_{se}$ per phase is related to the actual turns $N_s$ per phase by

$$N_{se} = \frac{4}{\pi} k_w N_s \tag{31}$$

The stator current $I_s$ can now be related to the linear current density by

$$I_s = \frac{2\pi r K_s}{3(2N_s)} = \frac{4\ r}{3\ N_{se}} K_{1s} \quad \text{A} \tag{32}$$

stator current $I_s$ leads $I_f$ by the angle $\beta$.

A PM motor with surface-mounted magnets is essentially non- salient since the incremental permeability of the magnet material is approximately the same as air ($\mu_r \approx 1.05$). Thus, the magnetizing inductance $L_m$ of the motor has the same form as in an induction motor [7].

$$L_m = \frac{3\pi}{2p^2} \mu_o N_{se}^2 \frac{r\ell}{\ell_{ge}} \quad \text{H} \tag{33}$$

Note that the magnetizing inductance is inversely proportional to the effective length $\ell_{ge}$ between the stator teeth and the iron of the rotor core. Typically, this may be in the range of 5–10 mm for a PM motor in contrast with 0.5–1.0 mm for an induction motor. The magnetizing inductance of a PM motor may thus be an order of magnitude smaller than that of an induction motor of similar dimensions. The magnetizing inductance decreases rapidly as the number of poles is increased, a feature which is also characteristic of induction machines [4].

The stator resistance $R_s$ per phase can be derived from the stator winding loss, using eq. 18 and 27 to give

$$R_s = \frac{3\pi}{8} \frac{\rho_c \ell_c}{d_e r k_w^2} N_{1s}^2 \quad \Omega \tag{34}$$

The leakage inductance $L_L$ of a surface mounted Pm motor has components similar to those of an induction motor stator [4]. The dominant components of leakage inductance are the stator slot leakage and the stator end winding leakage. There is no component of rotor leakage inductance. The space harmonic inductance which is substantial in some induction machines is negligible since it is typically less than 2% of the magnetizing inductance which is itself relatively small in a PM motor. As a first approximation,

$$\frac{L_L}{L_m} \approx \frac{1.5p\ell_{ge}}{cr} \tag{35}$$

Since the eddy current part of the core loss has been assumed to be proportional to the square of the $B.\omega_s$ product, the loss can be represented in the equivalent circuit by a near-constant resistance $R_c$. Operationally this resistance has been connected across the total induced stator voltage in Figure 7(a) rather than across the magnetizing inductance $L_m$. This takes into consideration the fact that the flux densities in the teeth and the yoke are proportional to the total stator flux linkage which in turn is a space vector sum of the air gap and leakage flux distributions. The value of the eddy current resistance in per unit is the inverse of the per unit core loss [3, 8].

Calculations of voltage-current relations are simplified by use of the circuit of Fig. 6(b) where $L_M = \Delta L_m, I_F = I_f/\Delta$, and $\Delta = 1 + L_L/L_m$.

The limiting value $I_{sm}$ of the stator current may be related to the source current $I_f$ using eq.8, 30 and 32 as,

$$\frac{I_{sm}}{I_f} = \frac{\Delta\pi}{4\sin^2\alpha}\left(1 - \frac{B_D \ell_{ge}}{B_r \ell_m}\right) \tag{36}$$

A phasor diagram ignoring the stator resistance is shown in Fig. 6(c). For operation at the maximum torque condition, ie., $\beta = 90°$, the stator voltage is

$$V_s = \omega_s L_M I_F [1 + (I_{sm}/I_F)^2]^{1/2} \quad \text{V} \tag{37}$$

If maximum torque is to be maintained up to a mechanical speed of $\omega_b = (2/p)\omega_s$ rad/s, and the maximum available rms stator voltage is $V_{sm}$, the required number of stator turns per phase may be found using eq.25, 27 and 28 as

$$N_s = \frac{V_{sm}}{2k_w B_{1g} r \ell \omega_b [1 + (L_L/L_M)^2]^{1/2}} \tag{38}$$

For a two-layer winding, the actual number of turns must be adjusted to be an integral multiple of the product $pc$.

## VIII. Higher Speed Operation

With appropriate control of the stator current angle $\beta$ , the speed may be increased considerably beyond the value $\omega_b$. From eq. 36 it is observed that the stator current $I_s$ can have a maximum value which is comparable to that of the source current $I_F$. For operation with $\omega_{mech}$ greater than $\omega_b$, the current angle $\beta$ is increased beyond 90° so that a component of the stator current acts to reduce the flux density of the magnet. If $I_s$ is maintained equal to $I_F$ in magnitude, with constant stator supply voltage, and ignoring the small effect of stator resistance, the speed torque relation as the angle $\beta$ is varied is characterized by

$$T/\hat{T} = \sin\beta \tag{39}$$

and

$$\frac{\omega_{mech}}{\omega_b} = \sqrt{2} cos(\beta/2) \tag{40}$$

For example, the torque will be 0.5 T at a speed of 2.73 $\omega_b$.

## IX. Conclusion

Variable-speed PM drive motors using Nd-Fe-B magnets are capable of very high torque and acceleration, particularly in applications with a small duty factor. For example, a typical motor with a maximum torque of 400 N.m can achieve an acceleration in excess of 20,000 rad/s$^2$ if the duty factor is 5%.

This paper develops approximate relations for determining the major motor dimensions to meet a design specification of transient mechanical output. These relations are useful in obtaining an estimate of what can be achieved before detailed motor design is carried out. Most of the design relations are expressed in a form which is independent of the characteristics of the inverter supply to the motor. It is only at the end of the

preliminary design process that the stator turns are chosen to match the motor to the inverter.

For intermittent operation, the stator current may be made comparable in magnitude to the equivalent source current of the magnet. This feature provides for a large maximum torque up to a base speed and also for operation at considerably higher speeds with somewhat reduced torque.

## REFERENCES

[1] T. Sebastian, G. R. Slemon, M. A. Rahman, "Design Consideration for Variable Speed Permanent Magnet Motors," *Proceedings, International Conference on Electrical Machines,* Part 3, pp. 1099–1102, Sept. 1986.

[2] T. Sebastian, G. R. Slemon, "Transient Torque and Short Circuit Capabilities of Variable Speed Permanent Magnet Motors," *IEEE Trans. Magnetics,* Vol. MAG-23, No. 5, pp. 3619–3621, Sept. 1987.

[3] Gordon R. Slemon, Xian Liu, "Modelling and Design Optimization of Permanent Magnet Machines," *Electric Machines and Power Systems,* Vol. 20, pp. 71–92, 1992.

[4] M. G. Say, *The Performance and Design of Alternating Current Machines,* (book), Pitman, 1948.

[5] E. Levi, *Polyphase Motors,* (book) John Wiley and Sons, New York, 1984.

[6] T. Sebastian, G. R. Slemon, "Transient Modelling and Performance of Variable Speed Permanent Magnet Motors," *IEEE Trans. Industry Applications,* Vol. IA-25, No. 1. pp. 101–107, Jan/Feb. 1989.

[7] G. R. Slemon, *Electric Machines and Drives,* (book), Addison Wesley, 1992.

[8] G. R. Slemon and L. Xian—Core Losses in Permanent Magnet Motors, *IEEE Transactions on Magnetics,* Vol. 26, No. 5, pp. 1653–1655, Sept. 1990.

**Gordon R. Slemon**, photograph and biography not available at the time of publication.